

We are IntechOpen, the world's leading publisher of Open Access books Built by scientists, for scientists

5,800

Open access books available

142,000

International authors and editors

180M

Downloads

Our authors are among the

154

Countries delivered to

TOP 1%

most cited scientists

12.2%

Contributors from top 500 universities



WEB OF SCIENCE™

Selection of our books indexed in the Book Citation Index
in Web of Science™ Core Collection (BKCI)

Interested in publishing with us?
Contact book.department@intechopen.com

Numbers displayed above are based on latest data collected.

For more information visit www.intechopen.com



Chapter

Minerals Observed by Scanning Electron Microscopy (SEM), Transmission Electron Microscopy (TEM) and High Resolution Transmission Electron Microscopy (HRTEM)

Taitel-Goldman Nurit

Abstract

Pictures from a scanning electron microscopy, transmission electron microscopy and high resolution microscopy are presented. Samples were collected from the marl layer in Judean Mountains in Israel, and the minerals observed were dolomite, calcite, goethite, and K-feldspar. In sands along the Mediterranean Seashore and the coastal plain in Israel, dark grains were rich in Ti, and quartz grains were covered by clays and hematite. Dust samples included clay minerals, Ti and Fe oxides. Iron oxides (goethite, akaganéite and lepidocrocite) were preserved within halite crystals at the Dead Sea area. In the Atlantis II and Thetis Deeps, in the central Red Sea, hot brines feel the deeps and minerals found in cores were magnetite, goethite, ferrosityte, manganite, todorokite, groutite and short range ordered ferrihydrite and singerite. Observation by electron microscopy enables us to see the size of euhedral or unehedral phases. Relations between the minerals are observed. Point analyses yield the chemical composition of the mineral with impurities, and Electron diffraction identifies the crystallography of the minerals.

Keywords: natural Fe, Ti, Mn oxides, quartz grains, euhedral, dolomite and K-feldspar

1. Introduction

The use of electron microscopy enables us to observe the size of minerals and understand their formation and the relations between various minerals in sediments. By using scanning electron microscopy (SEM), the size of minerals can be measured, morphology and relations between phases like coating or erosion of crystals can be observed. Using energy dispersive systems (EDS), the chemical composition of minerals can be obtained. The use of transmission electron microscopy (TEM) or high resolution transmission electron microscopy (HRTEM) enables us to measure the size of nanocrystals, obtain their chemical composition and identify the minerals formed.

With HRTEM, short range ordered phases can be identified and recrystallization of the minerals preserving initial morphology can be observed [1].

In this chapter, samples from various sites from Israel and the central Red Sea Deeps are presented and described. Rounded quartz grains arrive from the Nile River in Egypt to the Nile Delta, then are moved from the Delta with longshore current along the southeastern Mediterranean Sea to the Israeli coast. Moving of the grains to the coastal plain results from transgression and regressions of the sea causing the formation of sandstone ridges and soils [2]. The sand was also blown inland, forming sand dunes and eolianite calcareous sandstones ('kurkar').

Carbonate layers and marl or clay layers were formed during the Cretaceous period transgression of the Thetis Ocean. At the end of the Cretaceous, the layers were folded as part of the Syrian arc and the Judean Mountains were formed [3]. The maximum elevation of 1000 m separates between the western side of the mountains and the Judean desert on the eastern side.

The hypersaline terminate lake of the Dead Sea is located along the Dead Sea Transform fault at the eastern side of the Judean Mountains. The desert in the area causes evaporation of the Dead Sea water leading to elevated salinity of 340 g/l and precipitation of halite crystals [4].

Dust storms are common in Israel, mainly during autumn and spring. During the winter, dust storms appear at the early stage of rainstorms. The dust arrives either from North Africa from the Sahara desert or Saudi Arabia, depending on the weather cyclones [5]. The dust contains coarse silty quartz grains sourced from Sinai and the Negev in southern Israel [6].

The Atlantis II and Thetis Deeps are located in the central part of the Red Sea along the axial rift separating the Arabian and African plates. Hydrothermal brine discharges into the Deeps and the salinity results from dissolution of Miocene evaporates [7]. Elevated temperature results from interaction with hot magmatic and peridotite rocks, located underneath. Dissolved iron that is discharged from ultrabasic magmatic rocks, reacts with oxygen to form various phases of iron oxides. A narrow channel connects the southern Atlantis II Deep with small chain and discovery basins [8]. Drillings were performed during 'Mesada 3' expedition by Peussag company from Germany in the late 1970s and at the beginning of the 1980s as a part of the 'Saudi Sudanese Red Sea joint commission for exploring of red Sea Resources'. Samples were kept under 4°C in institut für meeresforschung (IFM) Geomar in Kiel, Germany [9].

2. Analysis of minerals

2.1 Mediterranean seashore sample

A sample from the southern part of the Mediterranean seashore was observed using scanning electron microscopy (SEM). The grains consist of transparent quartz grains (SiO₂) and black grains (**Figure 1**). The black grains were separated and checked using SEM and energy dispersive systems (EDS). It appears from the chemical analyses that these black grains are composed mainly of Ti-oxides.

2.2 Judean Mountains samples

Samples from the Judean Mountains in Israel were collected from layers of marl or clay. The samples were chipped or broken. The fresh surface was gold-carbonate

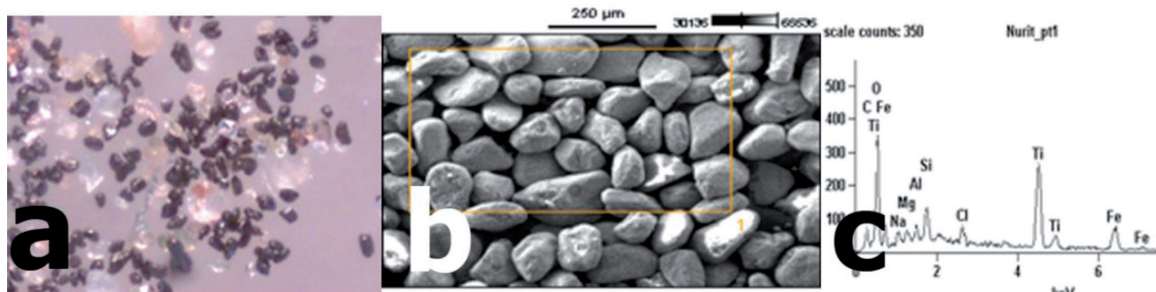


Figure 1. (a) Observation under the magnifying glass of sand from the southern part of the Israeli coast had transparent quartz grains and black grains, (b) SEM image of the black grains, and (c) chemical analyses of the black grains obtained by EDS, showing clays and Ti-oxide with iron impurity.

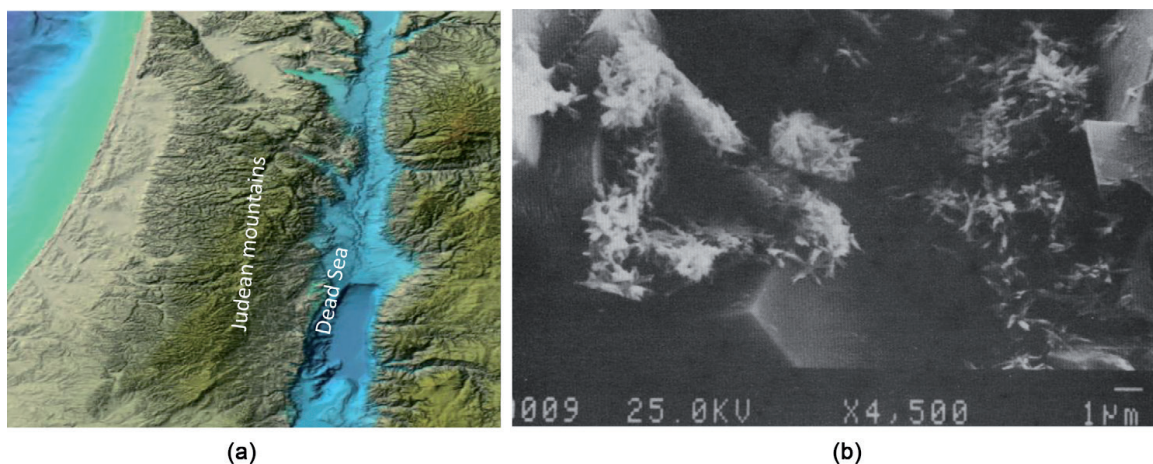


Figure 2. (a) Map of Israel with Judean mountains and the Dead Sea, and (b) SEM image of dolomite and goethite crystals from the Judean Hills in Israel.

coated for back-scattered mode on SEM and the chemical composition was established with EDS. By observing the samples, newly-formed minerals were identified by their euhedral morphology. Crystals of dolomite ($\text{CaMg}(\text{CO}_3)_2$) were identified

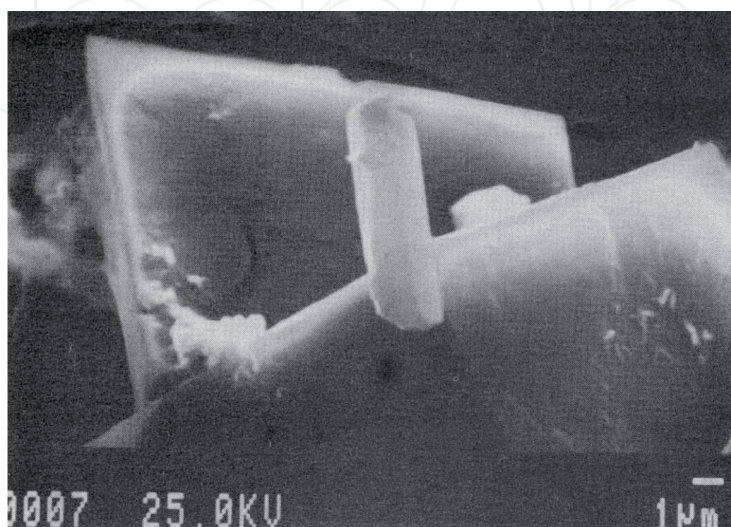


Figure 3. SEM image of idiomorphic shape of K-feldspar on euhedral dolomite crystals in marl layers of the Judean Hills in Israel.

in the argillaceous strata of the Judea group in the Judean Hills (**Figure 2**). The euhedral morphology indicates that they were formed in the marl layer. Goethite (FeOOH) crystals were formed later, filling the open spaces between the dolomite crystals.

In the marl layer K-feldspar, probably orthoclase or adularia (KAlSi_3O_8), was formed on euhedral dolomite crystals (**Figure 3**). Euhedral morphology of the K-feldspar indicates that it was formed in situ after dolomite crystallization [3]. Finding autogenic K-feldspar in the marl layers enabled measurement of the age of the layers [10].

Some of the dolomites in the Judean Hills were dissolved due to exposure to rains (**Figure 4**). The inner part was dissolved probably due to initial crystallization of dolomite with $\text{Ca/Mg} > 1$. As the dolomite crystallization continued, the outer part had a ratio of $\text{Ca/Mg} = 1$ so the dolomite was more stable. The dissolved inner part was later filled with calcite and clay minerals.

Crystallization of calcite (CaCO_3) along with clay minerals formed by agglutination of cyanobacteria caused formation of a tube (**Figure 5**).

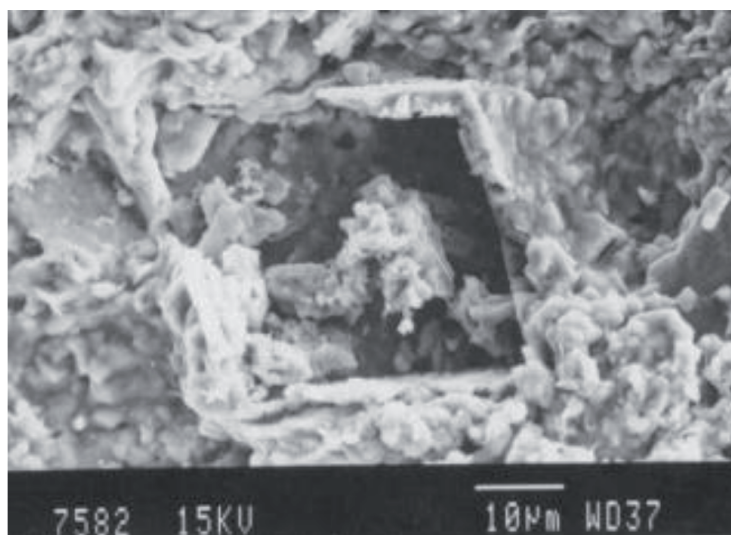


Figure 4.
SEM image of dolomite with inner part dissolved and outer part remained stable.

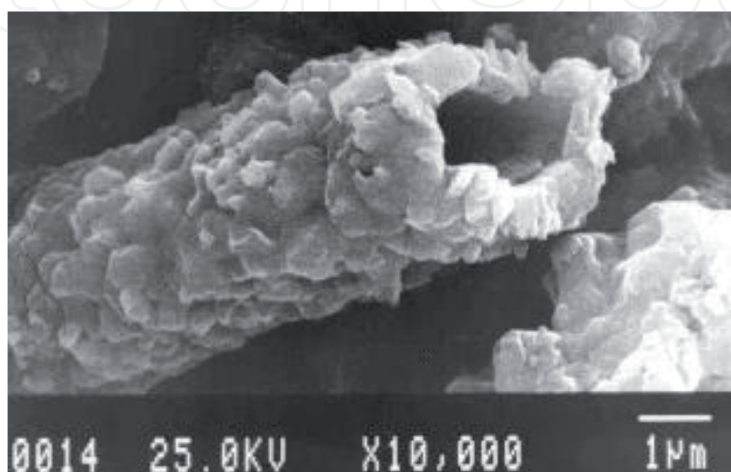


Figure 5.
SEM image of tube morphology of calcite and clays indicates biogenic origin and formation by cyanobacteria.

2.3 Samples from Red Sea deeps

Samples were collected from cores in the Atlantis II and Thetis Deep from the central Red Sea [9]. The sediments there were formed in a highly saline hydrothermal environment. Magnetite (Fe_3O_4) crystals were studied using SEM. They crystallized in the Thetis Deep located in the central Red Sea (**Figure 6**). Needles of goethite precipitate close to the magnetite. Point analyses measured on the magnetite yielded $\text{Si}/\text{Fe} = 0.01$ and impurities of V with $\text{V}/\text{Fe} = 0.002$ and Mn with $\text{Mn}/\text{Fe} = 0.002$.

Foraminifera's shells that originate from the upper part of the Red Sea sink and attach to the magnetite crystals.

Nano-sized particles (5–200 nm) were checked under transmission electron microscopy (TEM) using JEOL JEM-2100f analytical TEM operated at 200 kV, equipped with a JED-2300 T energy dispersive spectrometer (EDS) for microprobe elemental analyses. All chemical analyses were obtained by point analysis with a beam width of 1 nm JEOL. Crystalline phases were identified, using selected area electron diffraction (SAED) in the TEM.

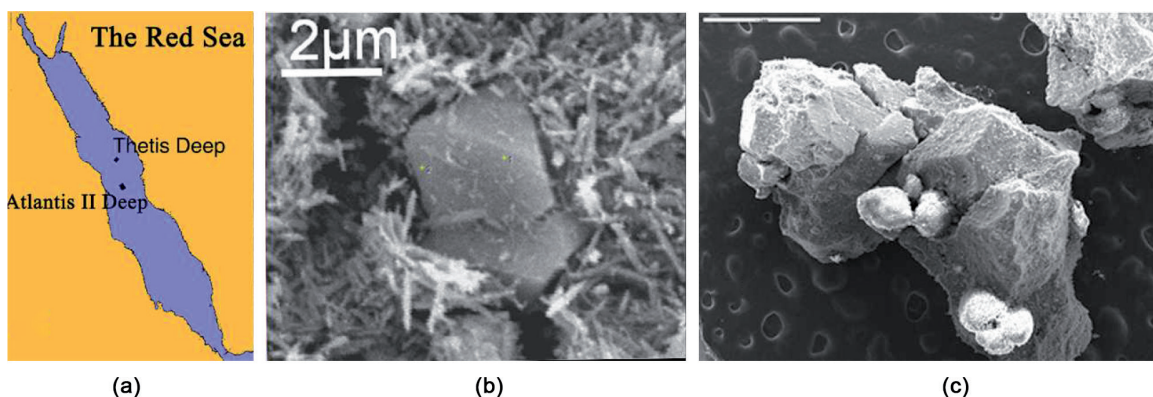


Figure 6. (a) Location of the Thetis deep and Atlantis II deep in the Red Sea, (b) SEM image of euhedral magnetite crystals surrounded by goethite crystals, and (c) SEM image of magnetite crystallized in the Thetis deep in the Red Sea with foraminifer's shells.

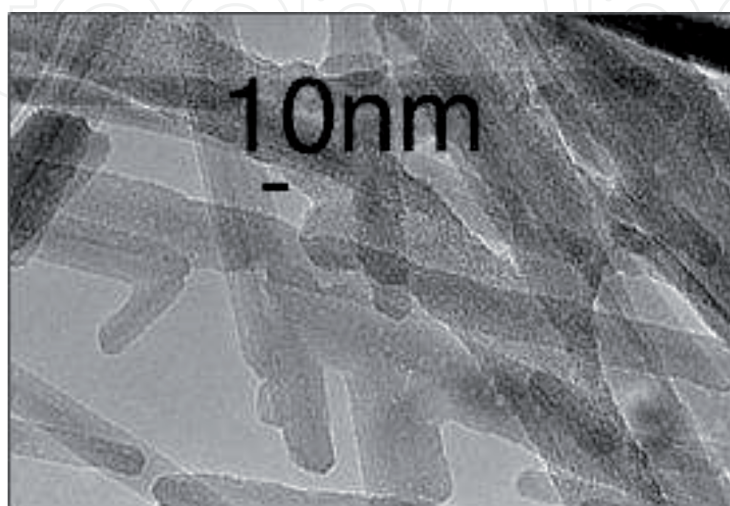


Figure 7. TEM image of mono-domain goethite with twinning from the Red Sea deeps due to elevated temperature. Goethite had an impurity of Si/Fe 0.02 atomic ratio.

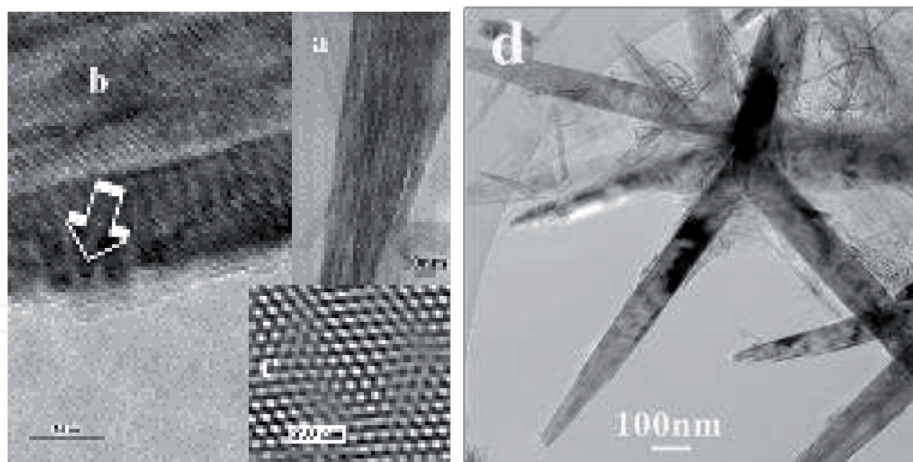


Figure 8. (a) HRTEM image of multi-domain goethite, (b) HRTEM image of the goethite, (c) fast Fourier transformation that shows the well-crystallized goethite, and (d) TEM image of goethite with twinning forming a star shape impurity of Si/Fe 0.04 atomic ratio.

Samples that were crystallized in the Red Sea Deeps had various morphologies due to salinity of the hydrothermal brines and their high temperature. Goethite (α -FeOOH) appears as mono-domain with twinning (**Figure 7**) or as multi-domain (**Figure 8**) and by high resolution, it is possible to observe well-crystallized phases. Impurity of Si in the goethite crystals was observed within the crystals: Si/Fe = 0.1 in multi-domain phase and Si/Fe = 0.02 in mono-domain structure. Star shape had Si/Fe = 0.04. Crystallization of goethite occurred at the upper part of the hydrothermal brine due to iron that discharges from the Deep and oxygen from Red Sea deep water.

Tiny goethite crystals grow on groutite (α MnOOH) in a sample from the southern part of the Atlantis II Deep in the Red Sea [11]. Groutite and goethite are iso-structural; hence crystallization of goethite was favored (**Figure 9**).

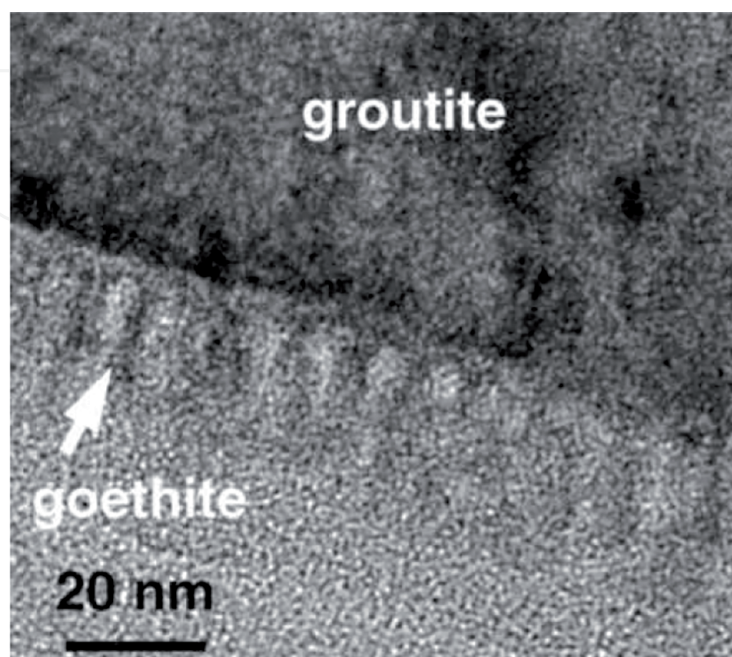


Figure 9. HRTEM image of goethite crystallized on groutite.

2.4 Samples from Dead Sea area and the Red Sea

In the Dead Sea area, colored halite can be observed with iron oxides preserved within halite crystals. Samples were studied using HRTEM [12]. Multi-domain akaganéite (β -FeOOH) (**Figure 10**) and multi-domain lepidocrocite (γ -FeOOH) (**Figure 11**) were crystallized in the area of the Dead Sea and then covered by halite crystals that preserved the initial phases.

Formation of akaganéite requires the presence of Cl^- ions, which had Si and Mn impurities ($\text{Si/Fe} = 0.06$, $\text{Mn/Fe} = 0.06$).

Lepidocrocite is crystallized at slow oxidation at $\text{pH} > 5$ and in the presence of chloride [12]. Plate morphologies of lepidocrocite were observed in Atlantis II and Discovery Deeps sediments in the Red Sea. Rod morphology was observed in sediments of the Thetis Deep in the Red Sea [9].

Formation of ferroxhyte (δ -FeOOH) requires high oxidation conditions [13]. Ferroxhyte was crystallized at the transition zone between the Red Sea deep water and the hydrothermal saline brine. Sample was collected from the upper part of sediments in the south-west basin of the Atlantis II Deep in the Red Sea. Ferroxhyte

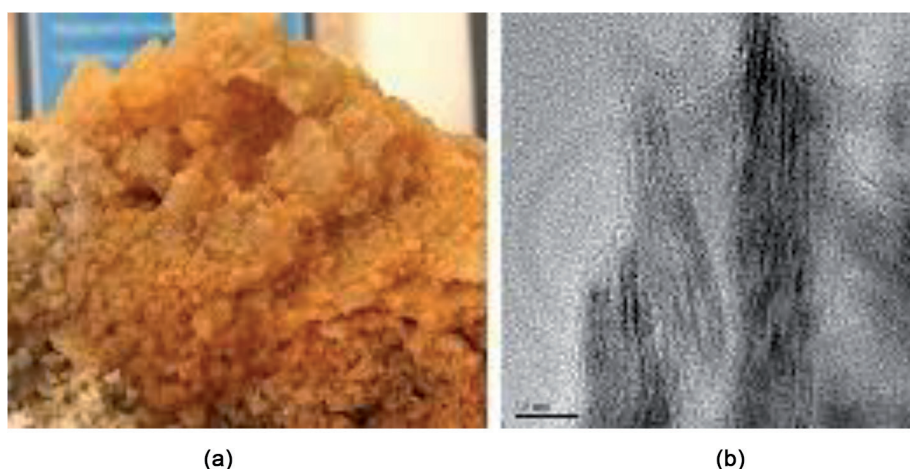


Figure 10. (a) Halite crystals from the Dead Sea area that include iron oxides, and (b) HRTEM image of multi-domain akaganéite (β -FeOOH) it contributes to the color of halite.

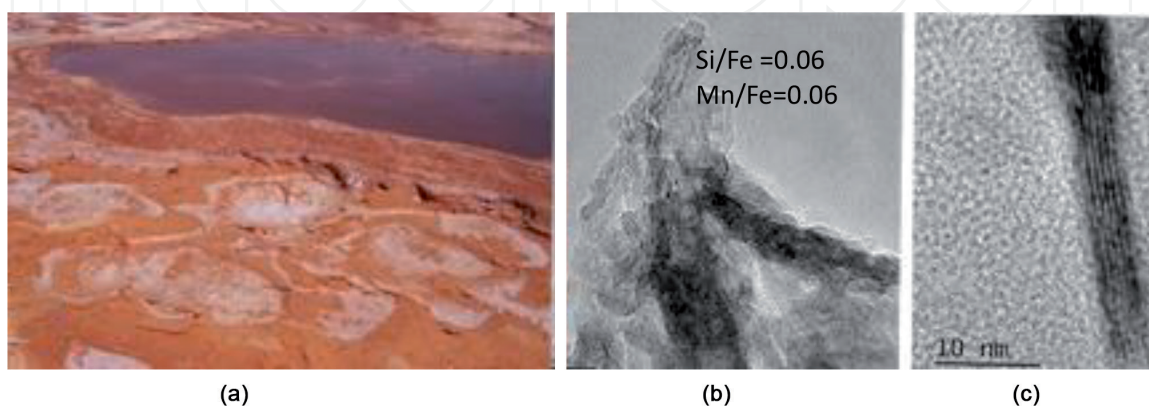


Figure 11. (a) Dead Sea area close to the seashore with halite that precipitates from the lake, (b) TEM image of lepidocrocite crystals that cause the color of the halite. Lepidocrocite crystals had impurities of $\text{Si/Fe} 0.06$ and $\text{Mn/Fe} 0.06$, and (c) HRTEM image of lepidocrocite preserved in the halite crystals.

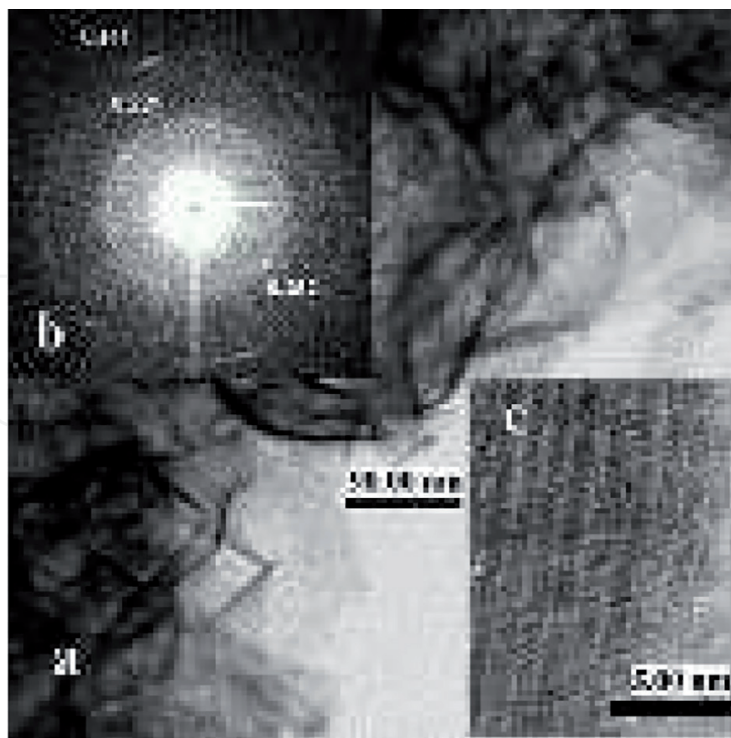


Figure 12. (a) HRTEM image of folded layers of ferroxhyte from the sediments of the Atlantis II deep, (b) Electron diffraction of ferroxhyte, and (c) HRTEM image shows a well-crystallized phase without dislocations.

appears as folded layers and a high resolution image shows that there are no dislocations in the crystals (**Figure 12**).

In the southern part of Atlantis II Deep in shallow water, Mn oxides were formed from the upper part of the brine. Minerals identified were todorokite $(\text{Ca},\text{Mg})_{1-x}\text{Mn}^{4+}\text{O}_{12} \cdot 3-4\text{H}_2\text{O}$, with impurities of $\text{Si}/\text{Mn} = 0.15$, $\text{Fe}/\text{Mn} = 0.28$. Manganite $\gamma\text{-MnOOH}$ had also an impurity of $\text{Si}/\text{Mn} = 0.10$ and $\text{Fe}/\text{Mn} = 0.20$ (**Figure 13**).

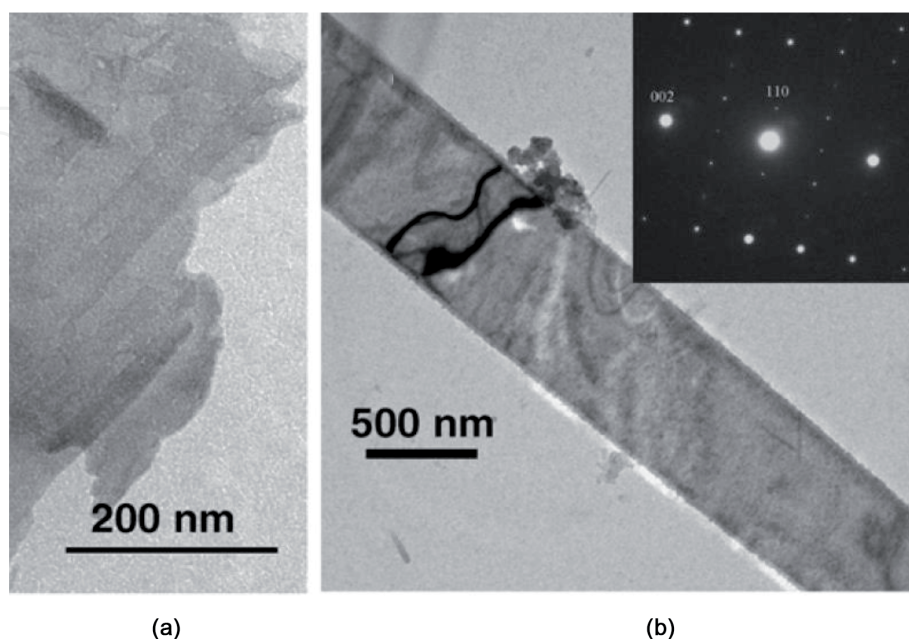


Figure 13. TEM images of Mn oxides from the southern part of the Atlantis II deep with Fe and Si impurities. (a) Todorokite $(\text{Ca},\text{Mg})_{1-x}\text{Mn}^{4+}\text{O}_{12} \cdot 3-4\text{H}_2\text{O}$, and (b) manganite $\gamma\text{-MnOOH}$, with electron diffraction.

Similar phases were also identified in the Chain and Discovery Deeps close to the Atlantis II Deep in the Red Sea [11].

2.5 Samples from the coastal plain of Israel

Quartz grains are dominant in soils on the coastal plain of Israel. Clay minerals, kaolinite ($\text{Al}_2\text{Si}_2\text{O}_5(\text{OH})_4$), montmorillonite ($(\text{Al}_2\text{Mg}_3\text{Si}_4)_{10}(\text{OH})_2\text{nH}_2\text{O}$), which arrive in the area as dust storms, cover the well rounded quartz grains. Iron oxides, mainly hematite (Fe_2O_3) crystals, are attached to the clay minerals and contribute to the red color of the red sandy soils (**Figure 14**).

2.6 Dust samples of Israel

Dust storms are common in Israel, (**Figure 15**). Dust samples were collected and studied with TEM. Most of the samples contain clay minerals, mainly montmorillonite, kaolinite and small amounts of illite. Nano-sized iron and titanium oxides are

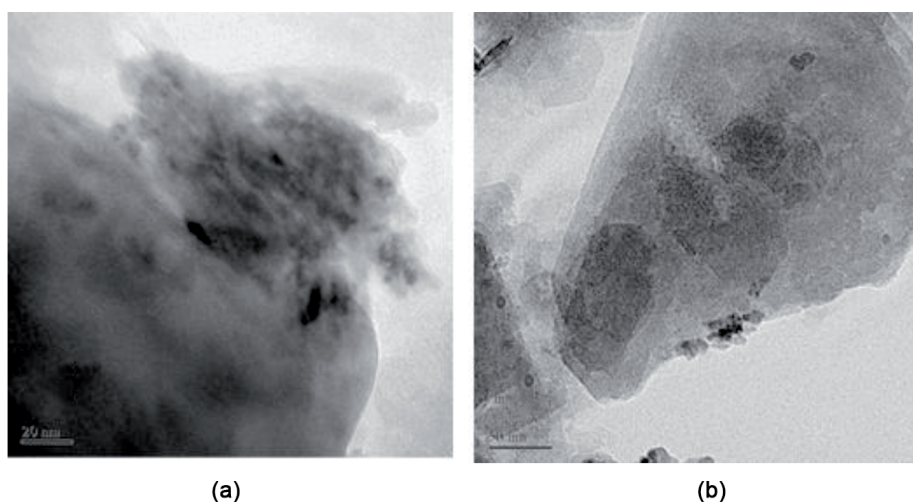


Figure 14.
(a and b) TEM images of rounded quartz grains covered by kaolinite and hematite in red sandy soil.

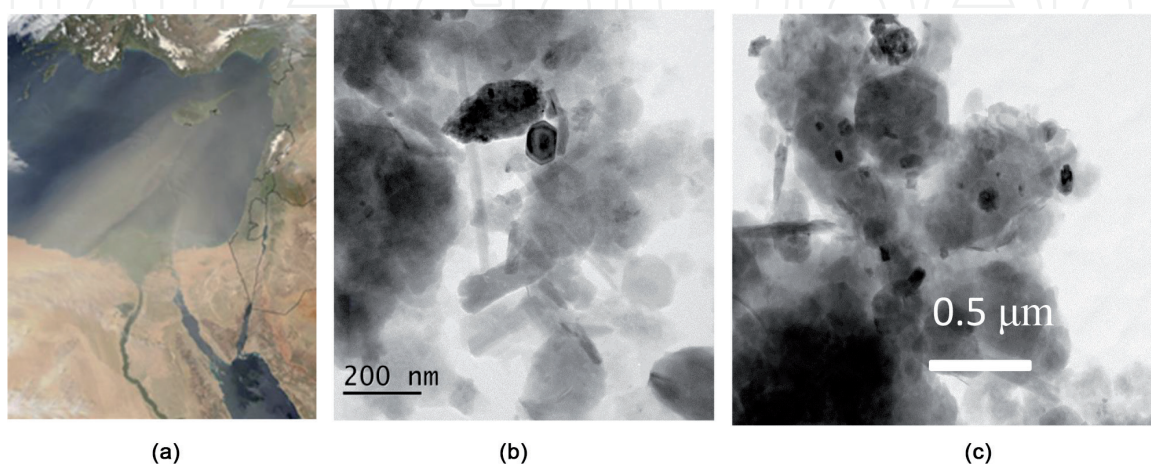


Figure 15.
(a) Dust storm in the Middle East, (b) TEM image of well-crystallized rutile that was identified in the dust along with clays and hematite, and (c) HRTEM image of dust samples made of clay minerals mainly montmorillonite and kaolinite. Hematite, ilmenite and Ti oxides are attached to the clays.

attached to the clay minerals forming clusters. The dust also covers quartz grains in sand dunes along the Mediterranean seashore and colors them into darker colors.

2.7 Short range ordered phases

HRTEM enables observation of short range ordered phases. Ferrihydrite ($\text{Fe}_5^{3+}\text{HO}_8\cdot 4\text{H}_2\text{O}$) and singerite ($\text{SiFe}_4\text{O}_6(\text{OH})_4\cdot \text{H}_2\text{O}$) were observed using HRTEM. The size of the ferrihydrite is around 5 nm in samples from the Atlantis II Deep and it has a hexagonal outline. Ferrihydrite from the Dead Sea forms clusters. In both samples, the use of high resolution enables us to see that the phase is short range ordered (**Figure 16**).

Formation of Ferrihydrite is at fast oxidation and $\text{pH} > 2$. Si serves as an impurity in the phase. With time, ferrihydrite can recrystallize into more stable iron oxides like hematite, akaganéite or goethite (**Figure 17**).

In the upper layer of sediments of the Atlantis II Deep in the Red Sea, a new short range ordered phase was observed using HRTEM. The new phase has disc morphology with well-crystallized margins and short range ordered inner part and it was named singerite ($\text{SiFe}_4\text{O}_6(\text{OH}_4\cdot \text{H}_2\text{O})$) (**Figure 18**) [14]. Singerite was formed by mixing of the highly saline hydrothermal brine that discharges into the Deep and Red Sea

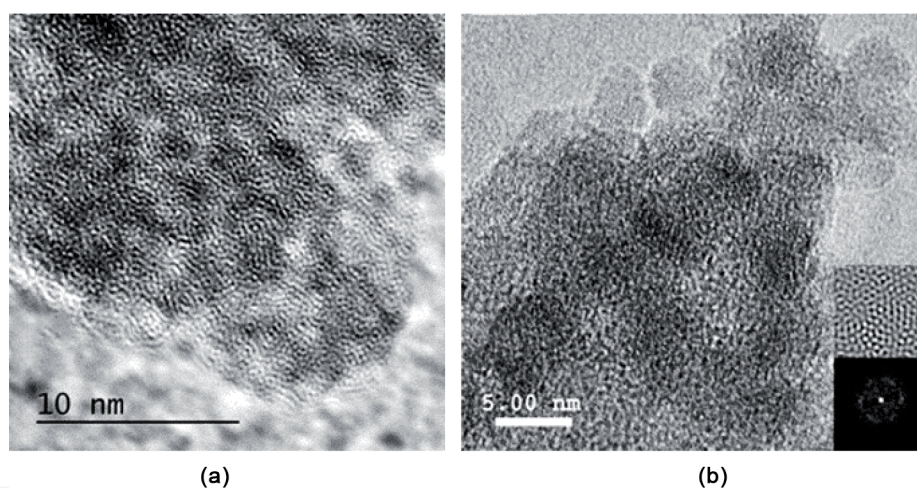


Figure 16. (a) HRTEM image of short range ordered ferrihydrite from the area of the Dead Sea, and (b) HRTEM image of ferrihydrite from Atlantis II deep with electron diffraction and fast Fourier transformation obtained by digital micrograph (Gatan) software.

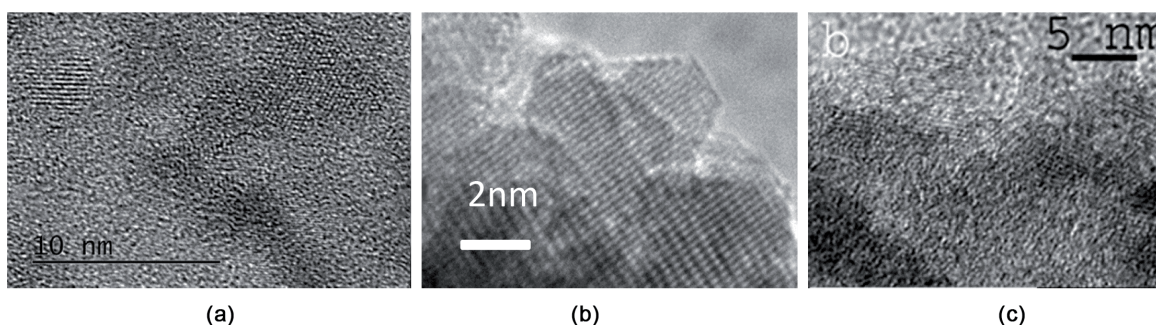


Figure 17. HRTEM images of samples from the Dead Sea area formed by recrystallization of ferrihydrite: (a) well-crystallized hematite, (b) well-crystallized akaganéite, and (c) well-crystallized goethite.

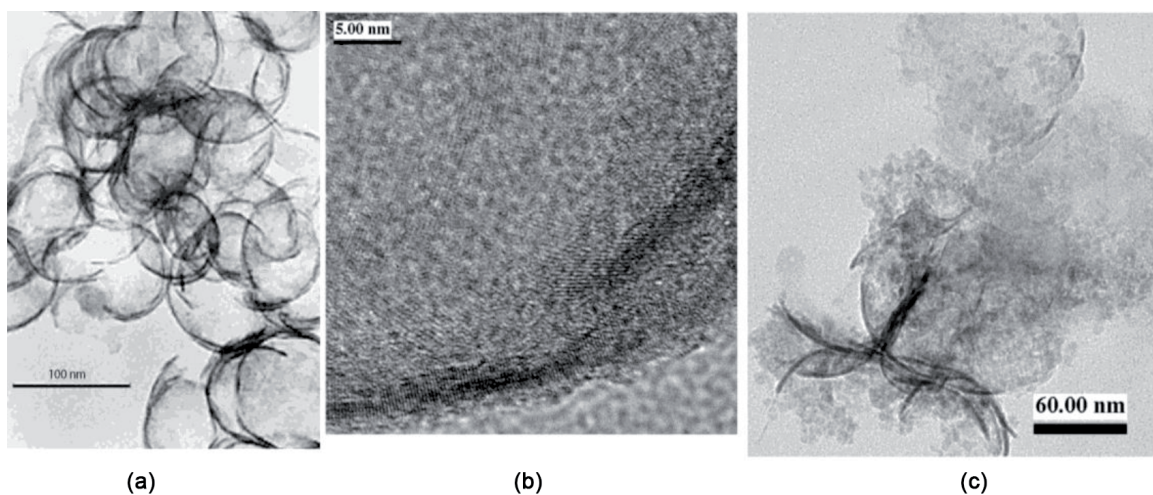


Figure 18. (a) HRTEM image of a cluster of rounded plates from the Atlantis II deep, Red Sea, (b) high resolution image of singerite with well crystallized outer part and short range ordered inner part, and (c) HRTEM image of recrystallization of singerite into clay mineral, probably nontronite.

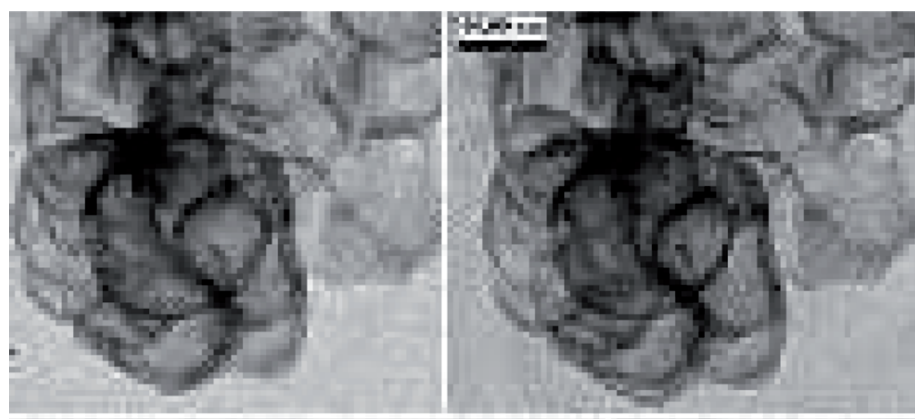


Figure 19. HRTEM image of a cluster of singerite. A small tilt of the sample enables us to see that singerite is made of rounded plates.

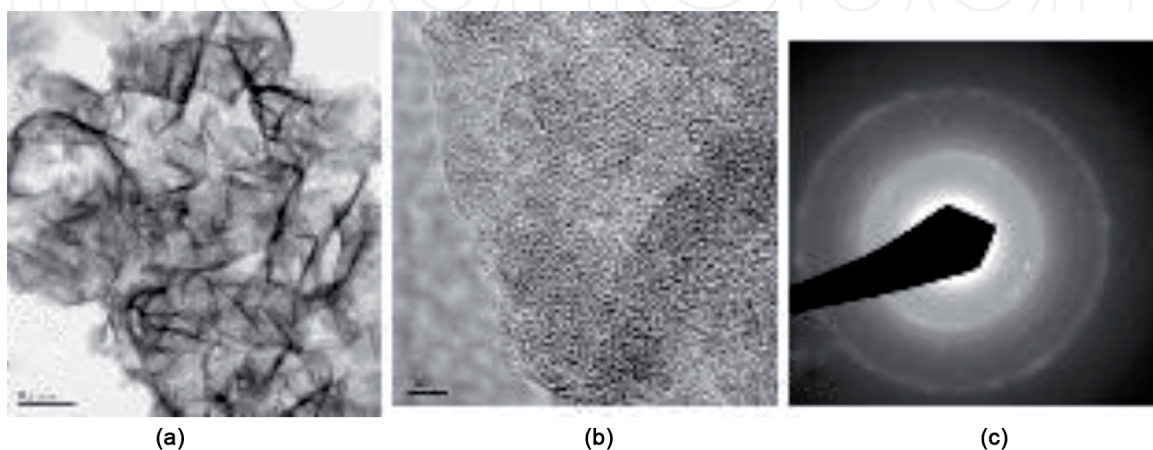


Figure 20. (a) HRTEM image of a cluster of mineraloid of Si, Fe Mn oxihydroxide, (b) HRTEM image showing short range ordered phase, and (c) Electron diffraction shows values of 0.255, 0.22 and 0.149.

deep water. With time, singerite recrystallizes into clay minerals, usually nontronite (iron-rich smectite). Hence singerite was found only in the upper layer of sediments in the Deeps. A similar rounded phase was synthesized under saline hydrothermal conditions [9].

A small tilt of the singerite sample enables us to see that singerite is a round plate (**Figure 19**).

A new short range ordered phase from Red Sea deeps: Mn-singerite?
 $\text{Si}(\text{Fe},\text{Mn})_4\text{O}_6(\text{OH})_4\text{H}_2\text{O}$ electron diffraction yielded 0.255, 0.22 and 0.149 (**Figure 20**).

3. Discussion

Observation of minerals under electron microscopy enables observation of well-crystallized phases, study of their chemical composition and finding of impurities in the crystals by using point analyses. Under HRTEM nano-sized short range ordered phase like ferrihydrite and singerite can be observed. A new phase Mn-singerite was also observed under HRTEM. Observation of twinning that results from the conditions in which the crystals were formed, such as salinity, pH, temperature, contributes to understanding the conditions in which formation of crystals occurred. Goethite for example appears as mono-domain, multi-domain crystals or twinning creating star shape morphology. Identification of the crystallography of the minerals observed was used by electron diffraction in transmission electron microscopy. Well-crystallized minerals with euhedral morphology indicate that they were formed in situ like samples covered by halite in the Dead Sea area. It is also possible to see the initially formed dolomite minerals and later another phase, goethite, filling the open space or attached to the initially formed phases. Goethite is also crystallized on groutite since both are isostructural.

Rounded morphology is formed due to pounding as the minerals moved from their initial location where they had crystallized to the new site. Quartz grains were observed along with Ti-rich minerals with rounded morphology as well. Other rounded quartz grains were observed in red sandy soils. Using electron microscopy enables us to see Nano-size phases that form a cluster of different minerals like clusters of dust. Clays are the main phases and iron or titanium oxides are captured between the clay layers or are adsorbed on their surfaces.

4. Conclusion

In this chapter Fe-oxides, Mn-oxides, Ti-oxides, quartz, dolomite, clays and K feldspar were studied using various electron microscopies (SEM, TEM and HRTEM). Using these methods helped to identify the crystallography, morphology and chemical composition of the minerals. Nano-sized short range ordered phases like ferrihydrite and singerite were also observed and identified.

Acknowledgements

Thanks to the Hebrew University of Israel for funding part of the research.

Thanks to Vladimir Ezersky from Ilse katz institute in Ben Gurion University in Israel for using TEM and HRTEM.

The research of the Dead Sea was supported by the Open University grant no. 100975.

IntechOpen


IntechOpen

Author details

Taitel-Goldman Nurit
The Open University of Israel, Raanana, Israel

*Address all correspondence to: nurittg@hotmail.com

IntechOpen

© 2022 The Author(s). Licensee IntechOpen. This chapter is distributed under the terms of the Creative Commons Attribution License (<http://creativecommons.org/licenses/by/3.0>), which permits unrestricted use, distribution, and reproduction in any medium, provided the original work is properly cited. 

References

- [1] Nurit T-G. Recrystallization Processes Involving Iron Oxides in Natural Environments and in Vitro, INTECH Recent Developments in the Study of Recrystallization. In: Wilson P, editor. 2013. pp. 163-174. ISBN: 978-953-51-0962-4
- [2] Arieh S. The Soils of Israel. Berlin Heidelberg: Springer-verlag; 2007
- [3] Nurit T-G, Lisa H-K, Eytan S. Clay minerals and feldspars in argillaceous strata of the Judea Group in the Jerusalem Hills. *Israel journal of Earth Science*. 1995;**44**:71-79
- [4] Avraham S, Amitai K. The story of saline water in the Dead Sea rift – The role of runoff and relative humidity. In: Garfunkel Z, Ben Avraham Z, Kagan E, editors. *Dead Sea Transform Fault System: Reviews* Springer. Dordrecht, Heidelberg, New York, London: Springer; 2014. pp. 317-353
- [5] Ganor E, Foner HA, Brenner S, Neeman E, Lavi N. The chemical composition of aerosols settling in Israel following dust storms. *Atmospheric Environment*. 1991;**254**(12):2665-2670
- [6] Rivka A, Yehouda E, Onn C. Quaternary influx of proximal coarse-grained dust altered circum-Mediterranean soil productivity and impacted early human culture. *Geology*. 2021;**49**:61-65
- [7] Manheim FT. Red sea geochemistry Init. 1974. pp. 975-998
- [8] Hartmann M, Scholten JC, Stoffers P, Wehner F. Hydrographic structure of brine filled deeps in the Red Sea – New results from Shaban, Kerbit, Atlantis II and discovery deep. *Marine Geology*. 1998;**144**:311-330
- [9] Nurit T-G. Nano-Sized iron-Oxides and Clays of the Red-Sea Hydrothermal Deeps. Characterization and Formation Processes. Saarbrücken, Germany: VDM Verlag Dr. Müller Aktiengesellschaft & Co KG; 2009
- [10] Gideon S, Kapusta Y, Amir S, Peter K. Sedimentary K-Ar signatures in clay fractions from Mesozoic marine shelf environments in Israel. *Sedimentology*. 1995;**42**(6):921-934
- [11] Nurit TG, Vladimir E, Dimitry M. High-resolution transmission electron microscopy study of Fe-Mn oxides in the hydrothermal sediments of the Red Sea deeps system. *Clays and Clay Minerals*. 2009;**57**(4):465-475
- [12] Nurit T-G, Vladimir E, Dimitry M. Nano iron oxides in the Dead Sea area. *Journal of Earth Science*. 2016;**2**:94-104
- [13] Rochelle C, Udo S. The iron Oxides, Structure, Properties, Reactions, Occurrences and Uses. New York: VCH Weinheim; 1996. p. 573
- [14] Nurit T-G. Crystallization of Fe and Mn oxides-hydroxides in saline and hypersaline environments and in vitro. In: *Advanced Topics in Crystallization*. Rijeka: Intech; 2015. pp. 323-339